JGR Biogeosciences

RESEARCH ARTICLE
10.1029/2018JG004908

Special Section:
Carbon Cycling in Tidal Wetlands and Estuaries of the Contiguous United States

Parameterizing Air-Water Gas Exchange in the Shallow, Microtidal New River Estuary

Bryce R. Van Dam[1,2,3], James B. Edson[4], and Craig Tobias[5]

[1]Institute of Coastal Research, Helmholtz-Zentrum Geesthacht, Geesthacht, Germany, [2]Department of Biological Sciences, Florida International University, Miami, FL, USA, [3]Institute of Marine Sciences, University of North Carolina at Chapel Hill, Chapel Hill, NC, USA, [4]Woods Hole Oceanographic Institution, Woods Hole, MA, USA, [5]Department of Marine Sciences, University of Connecticut, Groton, CT, USA

Abstract Estuarine CO_2 emissions are important components of regional and global carbon budgets, but assessments of this flux are plagued by uncertainties associated with gas transfer velocity (k) parameterization. We combined direct eddy covariance measurements of CO_2 flux with waterside pCO_2 determinations to generate more reliable k parameterizations for use in small estuaries. When all data were aggregated, k was described well by a linear relationship with wind speed (U_{10}), in a manner consistent with prior open ocean and estuarine k parameterizations. However, k was significantly greater at night and under low wind speed, and nighttime k was best predicted by a parabolic, rather than linear, relationship with U_{10}. We explored the effect of waterside thermal convection but found only a weak correlation between convective scale and k. Hence, while convective forcing may be important at times, it appears that factors besides waterside thermal convection were likely responsible for the bulk of the observed nighttime enhancement in k. Regardless of source, we show that these day-night differences in k should be accounted for when CO_2 emissions are assessed over short time scales or when pCO_2 is constant and U_{10} varies. On the other hand, when temporal variability in pCO_2 is large, it exerts greater control over CO_2 fluxes than does k parameterization. In these cases, the use of a single k value or a simple linear relationship with U_{10} is often sufficient. This study provides important guidance for k parameterization in shallow or microtidal estuaries, especially when diel processes are considered.

Key Points:
- When assessed over annual scales, short-term pCO_2 variation, rather than k parameterization, overwhelms uncertainty in calculated CO_2 flux
- CO_2 fluxes generated from bulk transfer equations were significantly greater than those measured by eddy covariance
- Day-night differences in the wind speed versus k relationship can cause parameterized CO_2 fluxes to diverge when pCO_2 is relatively constant

Supporting Information:
- Supporting Information S1

Correspondence to:
B. R. Van Dam,
vandam.bryce@gmail.com

Citation:
Van Dam, B. R., Edson, J. B., & Tobias, C. (2019). Parameterizing air-water gas exchange in the shallow, microtidal New River estuary. *Journal of Geophysical Research: Biogeosciences*, *124*, 2351–2363. https://doi.org/10.1029/2018JG004908

Received 31 OCT 2018
Accepted 3 JUL 2019
Accepted article online 9 JUL 2019
Published online 27 JUL 2019

1. Introduction

Carbon dioxide and methane released from inland waters contributes significantly to the global carbon (C) cycle (Raymond et al., 2013; Tranvik et al., 2009). Carbon dioxide (CO_2) emissions from the U.S. East Coast estuaries are between 1.9 and 4.2 Tg C/year, which is approximately 39–105% of the total riverine C input to this coastal zone (Laruelle et al., 2017; Najjar et al., 2018). While estuaries play a significant role in regulating C exchanges across the coastal zone, estimates of air-water fluxes reported in the literature are often accompanied by large uncertainty statistics. This is in part due to the challenges in deriving long-term averages for CO_2 concentrations, which may span orders of magnitude or vary between oversaturation and undersaturation over the course of a single day (Cotovicz et al., 2015; Crosswell et al., 2017; Maher et al., 2015), across seasonal scales (Guo et al., 2009; Koné et al., 2009; Van Dam, Crosswell, Anderson, et al., 2018), and with the impact of extreme weather events (Crosswell et al., 2014; Evans et al., 2012; Van Dam, Crosswell, & Paerl, 2018). Uncertainty associated with the parameterization of gas exchange, and its physical forcing, also vexes the quantitative assessment of estuarine CO_2 emissions.

CO_2 flux across the air-water interface may be parameterized according to a mass transfer equation (equation (1)): $CO_2\text{Flux} = k \times K_0 \times \Delta C$, where ΔC is the air-water concentration gradient, K_0 is the gas-specific solubility, and k is a gas transfer velocity (Wanninkhof, 1992). While the three variables in this mass transfer approach each have their own uncertainty (calculation of K_o and measurement of ΔC), the largest source of error is related to the parameterization of gas transfer velocity (Frankignoulle et al., 1998; McGillis et al., 2001; Upstill-Goddard, 2006; Wanninkhof & Mcgillis, 1999). In deep, open water environments, wind forcing is known to be the dominant factor affecting k, which is generally parameterized solely as some nonlinear function of wind speed (Broecker & Peng, 1974; Edson et al., 2011; McGillis et al., 2001; Wanninkhof & Mcgillis, 1999; Wanninkhof et al., 2009). In rivers and streams, turbulence reaching the air-water interface is largely generated by friction with the bottom (Ho et al., 2016; Maurice et al., 2017;

Raymond & Cole, 2001; Zappa et al., 2007). Additional factors include variable fetch (Vachon & Prairie, 2013; Woolf, 2005), turbidity (Abril et al., 2009), wave breaking (Crosswell, 2015; Liang et al., 2013; Wanninkhof et al., 2009; Woolf, 2005), the presence of biological surfactants (Lee & Saylor, 2010; McKenna & McGillis, 2004; Pereira et al., 2016; Wanninkhof et al., 2009), waterside thermal convection (Andersson et al., 2017; MacIntyre et al., 2010; Podgrajsek, Sahlée, Bastviken, et al., 2014; Podgrajsek, Sahlée, & Rutgersson, 2014), and chemical enhancement of CO_2 exchange at high pH (Smith, 1985; Wanninkhof, 1992).

If CO_2 flux is directly measured, k can be derived by rearranging equation (1) as

$$k = \frac{CO_2 Flux}{K_0 \times \Delta C} \tag{1}$$

A more universal form of this equation may be assembled by normalizing k to a constant Schmidt number (ratio of kinematic viscosity to molecular diffusion in water for CO_2; Sc)

$$k_{600} = \frac{CO_2 Flux}{K_0 \times \Delta pCO_2 \times \left({}^{600}/_{Sc}\right)^{-0.5}} \tag{2}$$

where k_{600} is the gas transfer velocity at a Schmidt number of 600 and Sc is the Schmidt number at in situ temperature and salinity (Wanninkhof, 2014). Once k is determined in this manner, its relationship with environmental drivers like wind speed, can be assessed, allowing k to then be estimated from wind speed alone. Since many factors beyond wind speed affect k, parameterizations based solely on measured k versus wind may produce estimates of gas transfer velocity that vary over nearly an order of magnitude (Jiang et al., 2008; Mørk et al., 2014).

Given the wide array of factors that may at times influence the physics of gas exchange (e.g., bottom-driven turbulence, surfactants, water current, and turbidity) and the lack of sufficient data, the best (or only) choice available may be to simply assume a constant value for k (Abril et al., 2014; Borges et al., 2003; Table 2; Borges, 2005). Two meta-analyses published in the past 20 years on this topic emphasize that the lack of direct measurements of k significantly hampers our ability to parameterize air-water gas exchange in estuaries and that care should be given when choosing values of k, with respect to location-dependent controls on gas exchange (Raymond & Cole, 2001; Upstill-Goddard, 2006). While the physical factors driving gas transfer may be highly system specific, k parameterizations for shallow microtidal estuaries have not yet been developed. This is despite the fact that these estuaries are dominant features along the U.S. East Coast and contribute significantly to regional carbon budgets (Herrmann et al., 2015; Laruelle et al., 2017; Najjar et al., 2018). Many of these regional carbon budget assessments use wind speed-based gas transfer parameterizations developed for the open ocean, highlighting the question of whether these equations can be reliably applied to estuaries in which the physical drivers of gas exchange may be very different from the open ocean. As mentioned above, additional factors may complicate the use of oceanic k parameterizations in estuaries, especially those that are narrow and shallow, including bottom-driven turbulence and changes in fetch with wind direction. In this study, we combine waterside measurements of CO_2 partial pressure (pCO_2) with direct measurements of CO_2 flux using an eddy covariance (EC) approach to derive an estuary-specific k parameterization in a microtidal, lagoonal estuary, the New River estuary, NC, USA (NRE). Because the NRE is representative of many estuaries along the U.S. East Coast, we provide guidance regarding how these k parameterizations might be applied in other systems and at varying temporal scales.

2. Methods

2.1. In Situ Measurements

Between 19 May and 24 October 2017, EC and waterside pCO_2 measurements were made in the upper NRE in an effort to simultaneously constrain values of CO_2 flux, K_0, and ΔC, allowing k_{600} to be calculated according to equation (2). Equipment was deployed at the end of a ~100-m dock extending into the estuary, depicted in Figure 1. Five individual deployments took place over the 5-month long study period, which collectively provided 942 discrete half-hour records of pCO_2 and associated parameters. A membrane-based CO_2 sensor and data logger (C-sense, Turner Designs, USA) was used to record in situ pCO_2, while

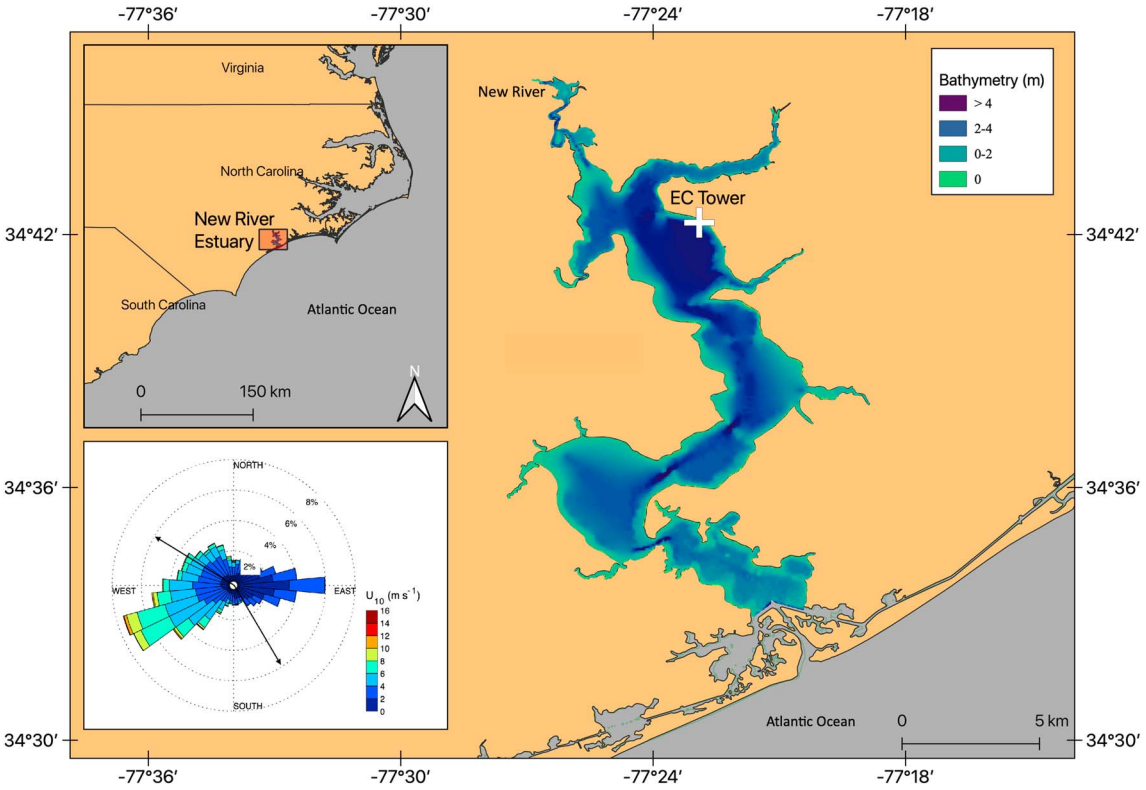

Figure 1. Site map showing location of the New River estuary and EC tower (34.70472°N 77.38170°W), including a wind rose of 10-min U_{10} data for the study period (19 May to 24 October 2017). Black arrows show wind directions for which CO_2 fluxes were calculated (130–290°). EC = eddy covariance.

dissolved oxygen (DO), water temperature (T_W), and salinity (Sal) were measured with a YSI-6600 (Yellow Springs, USA). The CO_2 sensor recorded pCO_2 with a manufacturer's indicated accuracy of 3% or 60 μatm. These in situ measurements were made at a depth of approximately 1 m, over intervals of 5 min (DO, Sal, and T_W) and 30 min (pCO_2). These high-frequency data were aggregated by hour to match the time scale of EC data.

2.2. EC

An EC system was deployed at the same location (34.70472°N, 77.38170°W), consisting of a sonic anemometer (WindMaster Pro, Gill Instruments Ltd., UK) and a closed-path CO_2 analyzer (LI-7200, LI-COR Biosciences, USA), recording three-component wind velocity and atmospheric CO_2 concentration, respectively, at a frequency of 10 Hz. The gas stream was dried using a Nafion gas drier, and the additional travel time associated with the increased tube length and dead volume in the drier was accounted for by adding a flow rate-dependent time lag to the CO_2 record. The accuracy of these measurements is ±1% and 1.5% of the reading, for CO_2 and wind speed, respectively. The measured horizontal wind component (at a height of 4.7 m) was shifted to a standard height of 10 m (U_{10}) following Large and Pond (1981). EC CO_2 flux was initially calculated at 10-min intervals then aggregated by hour in order to match the measurement frequency of waterside pCO_2 measurements.

2.3. EC Data Processing

In order to ensure that the EC flux footprint (Figure S1 in the supporting information; Kljun et al., 2015) was entirely over water, we excluded data where hourly average wind direction was outside of 130–290° (~58% of wind records). Favorable wind directions were encountered during much of the study period (Figure 1). In addition to screening by wind direction, data were also subject to Webb correction (Webb et al., 1980) and the removal of anomalously high and low k_{600} values (>40 or <−5 cm/hr), together accounting for 32% of hourly records. The high bound for k_{600} (40 cm/hr) was set at approximately 4 standard deviations (σ =

8.3 cm/hr) from the mean value (7.9 cm/hr), while the low bound was chosen to exclude measured CO_2 flux values that were drastically different in magnitude and direction from ΔpCO_2. Additionally, because ΔpCO_2 is in the denominator of equation (2), calculated k_{600} will approach infinity as ΔpCO_2 approaches 0; hence, values of ΔpCO_2 between −25 and +25 μatm were excluded from the analysis. Lastly, the relationship between calculated k_{600} and wind speed was assessed at 1.5 m/s bins of wind speed. This may be considered an arbitrary choice, but the choice of a 2-m/s bin size gave an unreasonably small number of bins (wind speed was generally low during the study period), while a 1-m/s bin size resulted in an insufficient number of measurements at high wind speed. The act of binning k_{600} by U_{10} removes the variability inherent in the unbinned data set and artificially inflates the correlation coefficient (r^2) yet remains a common practice (Borges et al., 2004; Cole & Caraco, 1998; McGillis et al., 2004; Prytherch et al., 2010; Wanninkhof & Mcgillis, 1999). Note that the k values presented here at a Schmidt number of 600 (k_{600}) can be converted to a CO_2-specific k (k_{CO2}) by $k_{CO2} = {k_{600}}/{(600/Sc_{CO2})^{0.5}}$.

3. Results and Discussion

3.1. CO_2 Fluxes

Surface water pCO_2 exhibited a strong diel signal, where maximum values generally occurred before dawn, and minima occurred in the late afternoon or early evening (Figure 2c). In many cases, pCO_2 transitioned from below equilibrium with the atmosphere to above over single diel cycles. This is in direct opposition to the thermodynamic effect of temperature-dependent solubility, which acts to increase pCO_2 during the day as water warms (Takahashi et al., 1993). This factor, in addition to the observation that DO and pCO_2 were strongly inversely related, indicates that biological processes of respiration and production controlled temporal variations in pCO_2. Air-water CO_2 exchange exhibited a similar diel signal, high at night (6.85 ± 12.6 $mmol \cdot m^{-2} \cdot hr^{-1}$) and low during the day (0.11 ± 10.8 $mmol \cdot m^{-2} \cdot hr^{-1}$). An EC footprint analysis (Kljun et al., 2015) indicates that the data screening steps were successful in limiting CO_2 flux measurements to those entirely within the aquatic domain, suggesting that adjacent forested and urban regions did not affect measured CO_2 flux (Figure S1). Averaged over the entire study period, CO_2 flux was 0.31 ± 1.4 $mmol \cdot m^{-2} \cdot hr^{-1}$, nearly half of the 0.68 average reported in Van Dam, Crosswell, Anderson, et al. (2018) for the New River estuary and within the range reported in Crosswell et al. (2017) for 2013–2014 and 2014–2015 (−0.023 and 2.3 $mmol \cdot m^{-2} \cdot hr^{-1}$, respectively) for the same estuary. Winds were generally moderate, not exceeding 14 m/s as a 30-min average and were dominated by a sea breeze, land breeze oscillation (Figure 1d). Similar to measured CO_2 flux, wind speed exhibited a diel pattern, high during the late afternoon and low at night. Likewise, maximum wind speed typically occurred during the afternoon, when ΔpCO_2 was lowest, enhancing CO_2 uptake during these hours.

3.2. Wind-Based Gas Transfer Velocity Parameterization

Calculated gas transfer velocity, k_{600}, was 9.37 (±9.47) cm/hr as an average over the entire study period, well within the range of what would be expected from parameterizations derived from the literature (~2–20 cm/hr; Ho et al., 2006; et al., 2014), given our average U_{10} of (4.2 m/s). Average k_{600} was also close to the 8-cm/hr exchange coefficient chosen in Frankignoulle et al. (1998). In contrast to open ocean (Wanninkhof & Mcgillis, 1999; Wanninkhof et al., 2009) and other coastal estuarine gas transfer studies (Borges et al., 2004; Ho et al., 2011), the relationship between hourly average k_{600} and U_{10} (before data were binned by wind speed) was relatively weak (Table 1). Nevertheless, when data were placed into 1.5-m/s bins of wind speed, a significant and positive relationship between k_{600} and U_{10} appears. In this study, the k_{600} versus U_{10} relationship appears to be linear during the day but is best described by a second-order polynomial at night (Figures 3c and 3d). Over the range of $3 < U_{10} < 7$ m/s, both linear and nonlinear fits derived here are within the range of other parameterizations taken from the literature (Figure 4). However, our daytime fits generate relatively low k_{600} values at $U_{10} > 6$ m/s, and nighttime polynomial fits produce high k_{600} values at U_{10} less than ~3 m/s and greater than ~7 m/s. In fact, at $U_{10} < 3$ m/s, average k_{600} was significantly higher (paired t test, $p = 0.013$) at night (9.32 cm/hr) than during the day (5.03 cm/hr).

Hence, it is not surprising that correlations between U_{10} and k_{600} were significantly improved when separated by day and night (Figures 3c and 3d and Table 1). This phenomenon has been observed before in rivers (Berg & Pace, 2017), lakes (Crusius & Wanninkhof, 2003; Erkkilä et al., 2018; MacIntyre et al., 2010;

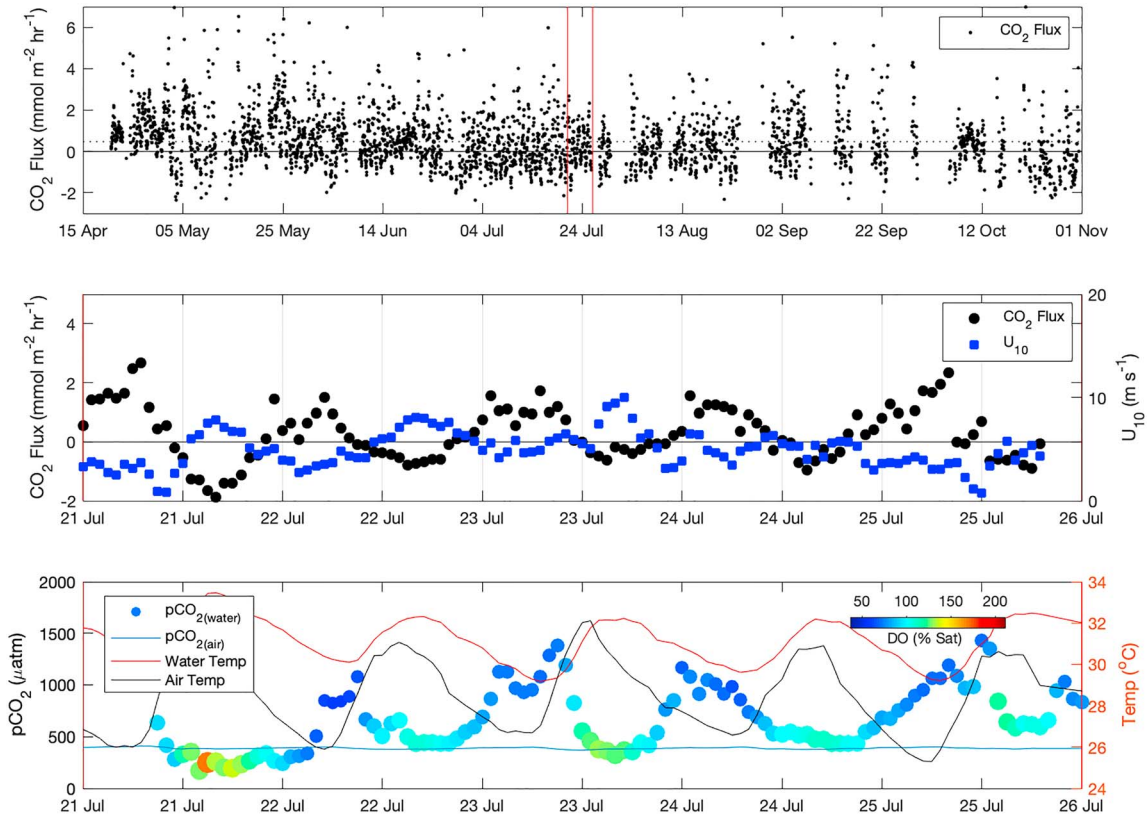

Figure 2. Time series plot of pCO_2 (µatm) over the entire study period (a), wind speed (m/s), and CO_2 flux (mmol·m^{-2}·hr^{-1}; positive values represent evasion of CO_2, as is common convention). (b) For one example sensor deployment period in July 2017, showing (c) surface water pCO_2 (µatm, colored by DO % saturation), atmospheric pCO_2, as well as water and air temperature, over the same time period. The horizontal black line in subplots (a) and (b) represents approximate air-water equilibrium with respect to pCO_2. The dotted line in (a) represents the long-term average of CO_2 flux (0.31 mmol·m^{-2}·hr^{-1}).

Podgrajsek, Sahlée, Bastviken, et al., 2014; Podgrajsek, Sahlée, & Rutgersson, 2014; Vachon & Prairie, 2013), reservoirs (Liu et al., 2016), high-latitude fjords (Andersson et al., 2017), and the open ocean (McGillis et al., 2004; Rutgersson et al., 2011). However, a literature search found no such effect documented in a representative midlatitude estuary. This day-night difference may be related to the stability of the air-water boundary layer. In concept, air-water gas exchange is limited by the size of the diffusive boundary layer (DBL), across which gas molecules must diffuse to pass through the air-water interface. Factors that add turbulence to the air-water interface can decrease the size of this DBL and accelerate gas exchange,

Table 1
Best Fit Equations (equations (1)–(6)) and R^2 Values for U_{10} (m/s) Versus k (cm/hr) Parameterization Shown in Figure 5

Aggregation Method	Day	Night	Combined
Binned	$k = 1.9\times U_{10} + 2.3$ $R^2 = 0.92$ (1)	$k = 18.5-(5.3\times U_{10}) + (0.64\times U_{10}{}^2) R^2 = 0.95$ (2)	$k = 1.5\times U_{10} + 4.2 R^2 = 0.78$ (3)
Unbinned	$k = 2.0\times U_{10} + 1.2 R^2 = 0.15$ (4)	$k = 11.7-(1.3\times U_{10}) + (0.14\times U_{10}{}^2) R^2 = 0.0072$[a] (5)	$k = 1.3\times U_{10} + 3.8$ $R^2 = 0.0694$ (6)

[a]The slope of the regression was not significantly different from 0 ($\alpha = 0.05$).

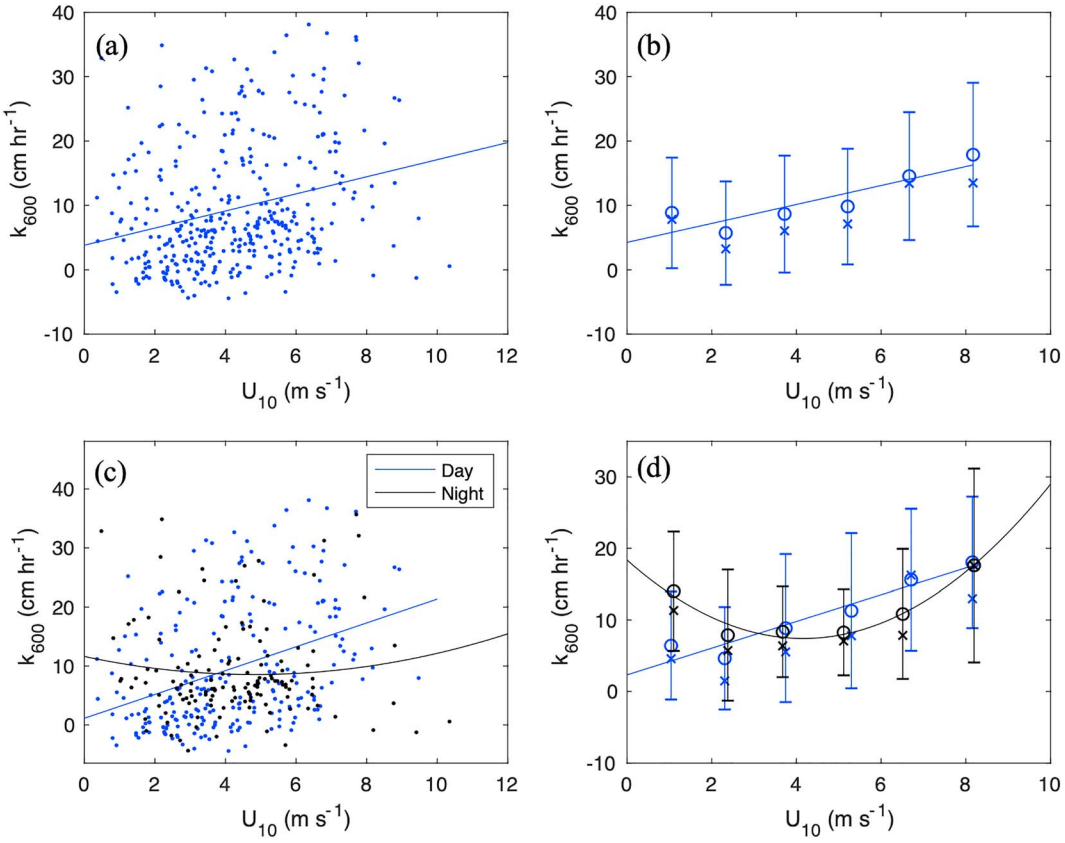

Figure 3. Relationship between U_{10} and k_{600}, showing (a) all data (equation (6)), (b) all data binned at 1.5-m/s intervals (equation (3)), (c) all data split by day (equation (4)) and night (equation (5)), and (d) binned day (equation (1)) and night (equation (2)). In subplots (b) and (d), the error bars represent standard deviation of k_{600} values in each bin of U_{10}. Mean and median k_{600} values for each bin are shown as "o" and "x" respectively.

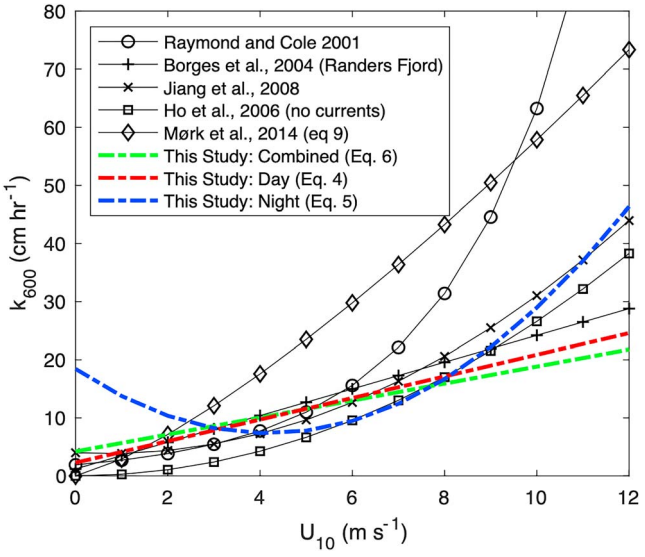

Figure 4. Literature comparison of gas transfer velocity parameterizations for estuaries, updated with the results of this study.

while those that expand the DBL will hamper gas transfer (Upstill-Goddard, 2006; Wanninkhof et al., 2009). Solar heating of the water surface can result in thermal stratification and a larger DBL, while the loss of heat to the atmosphere can create a "cool skin" at the water's surface, causing convective overturn, effectively decreasing the size of the DBL. In this manner, waterside convection can enhance gas exchange during the night or other times when net heat fluxes are toward the atmosphere (MacIntyre et al., 2010; Podgrajsek, Sahlée, & Rutgersson, 2014; Rutgersson et al., 2011). That this convective enhancement in k should be maximized at night, when pCO_2 is typically at a maximum (Figure 2c), means that the use of a single, linear k parameterization for both day and night data will likely cause mass transfer approaches to underestimate actual CO_2 fluxes.

3.3. Comparison of Measured and Modeled CO_2 Fluxes

In this study, we measured CO_2 flux directly using the EC technique and also measured surface water pCO_2, wind speed, temperature, and salinity, from which a mass transfer flux can be calculated by equation (1). Hence, we can compare these two independent determinations of CO_2 flux and assess the degree to which these approaches agree. In Figure 5a, the k model of Jiang et al. (2008) and the combined day-night model from this study (equation (3)) are plotted against CO_2 flux measured by EC. Modeled and measured CO_2 fluxes were clearly correlated, but these

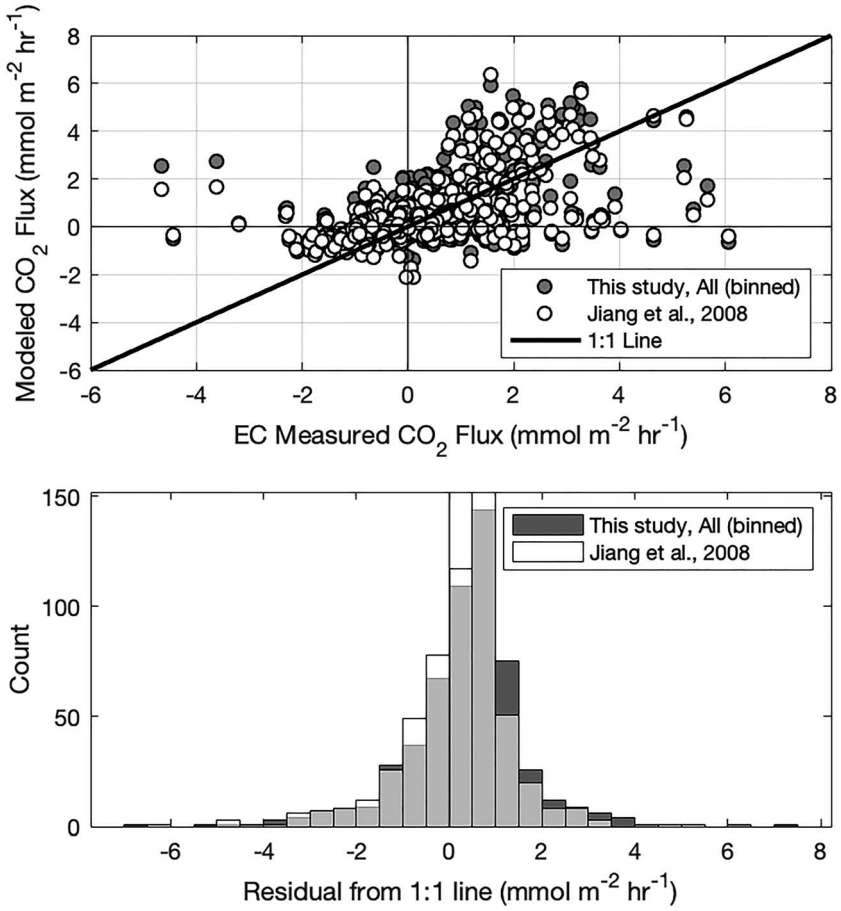

Figure 5. Relationship between hourly average measured (a) CO_2 flux (by EC) and CO_2 flux determined by a mass transfer model using the "combined and binned" k parameterization in Table 1. ($r^2 = 0.29$) and Jiang et al. (2008) ($r^2 = 0.30$). The slope between measured and modeled CO_2 flux was significantly different from 0 ($\alpha = 0.05$). (b) Histogram of residuals from the 1:1 line. EC = eddy covariance.

wind speed-based models could only explain 29% and 31% of the variance in measured flux, respectively (Figure 5a).

Furthermore, most of our points fall above the 1:1 line, indicating that the mass transfer approach involving these k parameterizations may overestimate CO_2 flux, relative to the flux measured by EC. The residuals from the 1:1 line (summarized in Figure 5b) represent the difference between CO_2 fluxes measured by EC and calculated from mass transfer equations and were 0.35 ± 1.3 mmol·m^{-2}·hr^{-1} (for the parameterization in equation (3)) and 0.21 ± 1.2 mmol·m^{-2}·hr^{-1} (for k calculated from Jiang et al., 2008). Averaged over the study period, CO_2 flux calculated using equation (3), (0.67 ± 1.3 mmol·m^{-2}·hr^{-1}) and Jiang et al., 2008 (0.52 ± 1.2 mmol·m^{-2}·hr^{-1}) were approximately twice the EC-measured CO_2 flux (0.31 mmol·m^{-2}·hr^{-1}). From this, we can infer that the mass transfer approach captures the sign of measured CO_2 flux but may overestimate its magnitude.

3.4. Effects of Convection on Gas Transfer Velocity

Because waterside measurements were collected in parallel with those from the EC tower, we were able to more closely examine the role of thermal mixing on measured k. Hence, to address effect of convective forcing on measured k_{600}, we first derived air-water buoyancy fluxes (Jeffery et al., 2007):

$$B = \frac{g \times a \times Q_h}{c_w \times \rho_w} + \frac{g \times \beta_s \times Q_l}{\lambda \times \rho_w} \tag{3}$$

where the buoyancy flux (B; m^2/s^3) is proportional to the total heat flux (Q_h), which is the sum of sensible

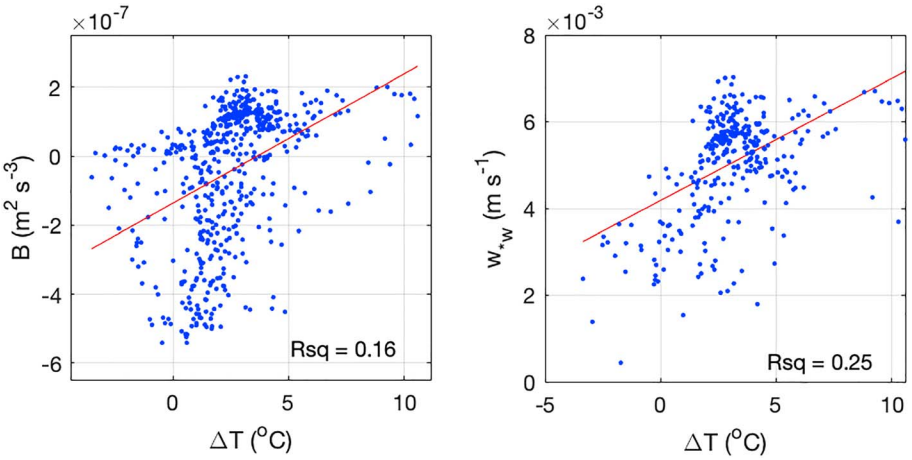

Figure 6. Relationship between air-water temperature gradient (ΔT; T_{water}-T_{air}) and buoyancy flux (a) and convective velocity scale (b). Both slopes are significantly greater than 0 ($\alpha = 0.05$).

and latent heat flux (Q_l) and longwave and shortwave radiation. Gravitational acceleration (g), latent heat of vaporization (λ), and specific heat of water (c_w) are constants, while thermal expansion (a), saline expansion coefficient (β_s), and water density (ρ_w) were calculated at in situ temperature and salinity using the GSW toolbox in Matlab (McDougall & Barker, 2011). By convention, when B is positive, water *loses* density to the atmosphere and becomes more buoyant and more stably configured, thereby increasing the distance through which gas must diffuse to exchange between the water and the atmosphere. When the surface layer *gains* density, buoyancy is lost (negative B), which in turn causes vertical mixing or at least shrinking of the DBL. Calculated B was then used to determine a waterside convective velocity scale (w_{*w}; m/s) following the approach of Jeffery et al. (2007) and MacIntyre et al. (2001)

$$w_{*w} = B \times h^{\frac{1}{3}} \tag{4}$$

where h is the mixed layer depth (assumed equal to the total water depth; 1.5 m). Hence, a larger buoyancy flux (B) or mixed layer depth (h) will result in increased convective overturning and a decrease in the waterside resistance to gas transfer.

As expected, both B and w_{*w} were positively correlated (Figures 6a and 6b) with the air-water temperature gradient (ΔT; T_{water}-T_{air}), such that the buoyancy flux was in the direction of the atmosphere, and waterside convection increased, as T_{air} fell below T_{water} ($R^2 = 0.17$ and 0.25 respectively, p value < 0.001). The air-water temperature gradient (ΔT) was significantly greater ($\alpha = 0.05$) at night (3.4 ± 2.2 °C) than during the day (1.9 ± 1.9 °C). Furthermore, w_{*w} was also positively correlated with U_{10}, and this relationship was strongest at night ($R^2 = 0.12$, p value < 0.001). However, no correlation was found between w_{*w} and measured k_{600} (Figure S3; $R^2 = 0.019$, p value $= 0.045$). This lack of relationship between w_{*w} and k_{600} is likely due to relatively low magnitude of w_{*w}, which never exceeded 0.0076, while the typical cutoff for "convective conditions" is often considered to be above $w_{*w} > 0.01$ (Andersson et al., 2017; Rutgersson et al., 2011).

Prior studies have assessed the relative importance of waterside convection and wind forcing on gas transfer by comparing w_{*w} and the airside friction velocity (u_{*w}), where the conditions are considered "convective" when the ratio of u_{*w}/w_{*w} falls below 0.75 (Andersson et al., 2017; Podgrajsek, Sahlée, & Rutgersson, 2014). We calculate u_{*w} according to MacIntyre et al. (2001), as $u_{*w} = (\tau/\rho)^{1/2}$ where τ is the measured wind stress and ρ is the density of water at in situ temperature and salinity. Because equation (4) is only valid for $B > 0$, calculated w_{*w} was not significantly different between night and day (p value = 0.54). However, u_{*w}/w_{*w} was below the convective threshold of 0.75 a total of 41% of the time during the night and only 21% of the time during the day. This suggests that while convection was not a major driver of k_{600}, it appears that some fraction of the nighttime enhancement of k_{600} at low wind speed may be attributable to convective collapse of the DBL. However, it remains likely that factors other than wind- or convection-driven turbulence affected k_{600} and may have played a role in increased nighttime k_{600}. One important such factor that was

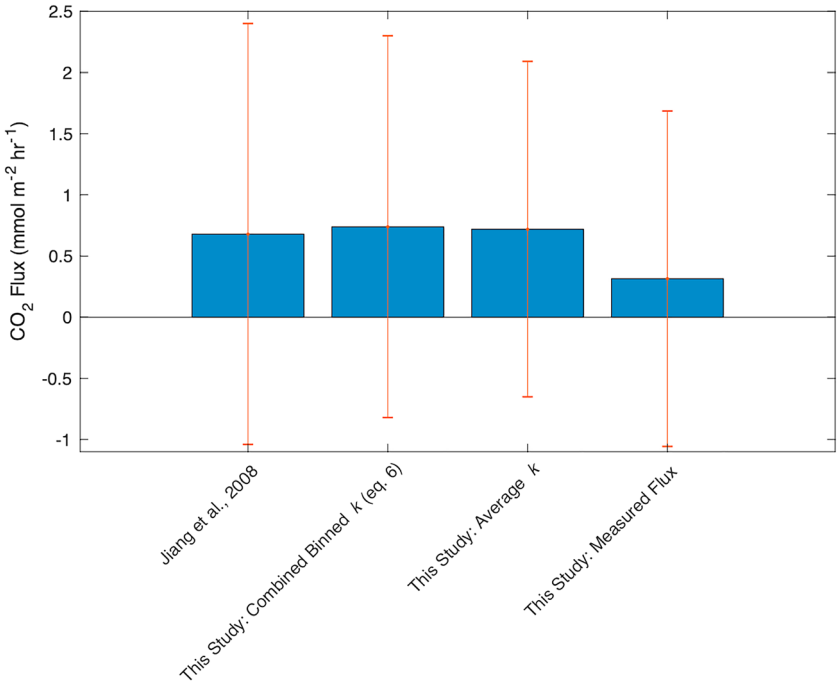

Figure 7. Average NRE CO_2 flux (2014–2016) with different k_{600} parameterizations. Jiang et al. (2008) used to derived the flux presented in Van Dam, Crosswell, Anderson, et al. (2018). Error bars represent the standard deviation of interpolated daily average CO_2 flux.

not accounted for in this study was bottom-driven turbulence, which has been shown to at times significantly enhance gas transfer velocity, particularly in shallow estuaries (Ho et al., 2016, 2018; Maurice et al., 2017; Raymond & Cole, 2001; Rosentreter et al., 2017; Zappa et al., 2007). Because the NRE is quite shallow (average depth <2 m), it is plausible that bottom-driven turbulence may have played an important role in enhancing k. While measurements related to water turbulence or velocity were not possible during the present study, such an investigation into bottom-driven turbulence remains an important avenue for future research.

3.5. Significance to Estuarine CO_2 Emissions

Prior studies show that CO_2 emissions from the NRE are small relative to other estuaries (−0.023 to 2.3 mmol C·m^{-2}·hr^{-1}) and vary with interannual changes in freshwater loading (Crosswell et al., 2017; Van Dam, Crosswell, Anderson, et al., 2018). Previous estimates in the NRE used identical waterside measurement methods to constrain air-water CO_2 gradients and to parameterize gas transfer. The k_{600} versus U_{10} parameterizations of Jiang et al. (2008) were used in both Crosswell et al. (2017) and Van Dam, Crosswell, Anderson, et al. (2018) because it represented a compilation of previous work and is thus a reasonable "middle of the road" k_{600} parameterization. In constructing a carbon budget for the NRE, Crosswell et al. (2017) ascribed the uncertainty in the air-water CO_2 exchange component to the upper and lower bounds of gas transfer using the k_{600} parameterizations of Prytherch et al. (2010) and Ho et al. (2006), respectively. It is important to note that all of these parameterizations were constructed for systems with different physical characteristics from the NRE. We reevaluated CO_2 exchange in the NRE, using the identical 2014–2016 data set from Van Dam, Crosswell, Anderson, et al. (2018) and comparing the effect of different k_{600} parameterizations (three from this study as well as Jiang et al., 2008). Figure 7 shows these results, where the height of the bar represents the average CO_2 flux (mmol·m^{-2}·hr^{-1}) determined using the indicated k_{600} parameterization, and the error bar indicates the standard deviations of daily average CO_2 fluxes, which were determined by linearly interpolating ΔpCO_2 measurements between sampling dates as described in Van Dam, Crosswell, Anderson, et al. (2018). None of the parameterizations derived in this study generate annual CO_2 fluxes that were

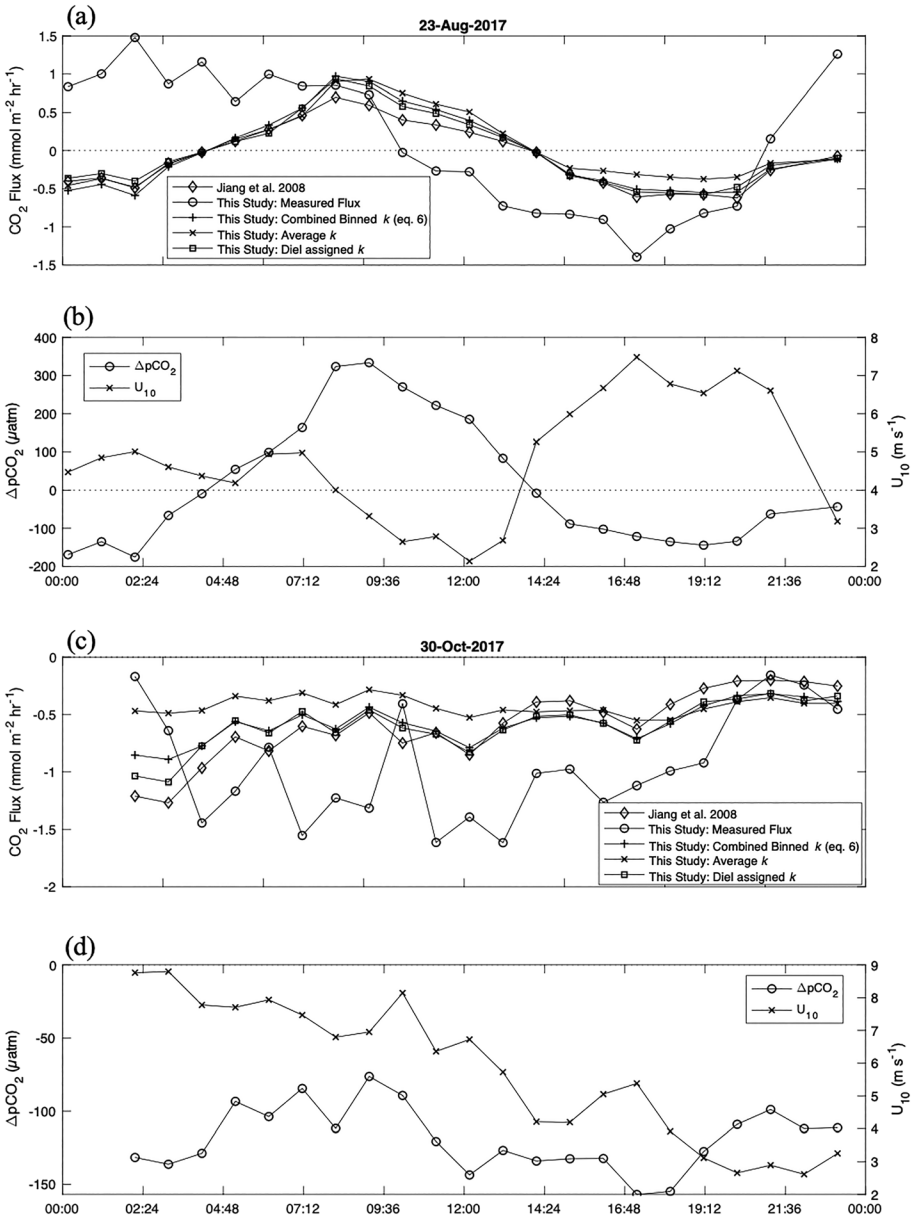

Figure 8. Time series plots of measured and modeled CO_2 flux (mmol·m^{-2}·hr^{-1}), as well as ΔpCO_2 (μatm) and U_{10} (m/s) for a typical summer day (a, b) and another day in which pCO_2 and wind speed were relatively stable (c, d).

significantly different from those calculated using the k_{600} parameterization of Jiang et al. (2008). Clearly, daily to seasonal variation in pCO_2, rather than gas transfer parameterization, overwhelms the uncertainty in calculated CO_2 emissions, when assessed on an annual scale. For example, the diel range in pCO_2 measured during this study was very high, often ~1,000 μatm, while the diel range in k_{600} was at most ~40 cm/hr. In fact, when fluxes were calculated from an average k_{600} (9.37 cm/hr), annual fluxes were not different from when our wind-based parameterizations were used (Figure 7). Hence, when long-term CO_2 flux estimates are desired for systems where wind speed data are limited or when no specific information exists regarding the physical forcing of gas transfer, it may be appropriate to calculate CO_2 fluxes from a single, average k value (provided that the variability in pCO_2 is sufficiently large). This is not to say that small-scale variations in k are not important; it is simply that the uncertainty due to these variations, in terms of U_{10} measurement and k fitting, tends to cancel out over longer time scales. This contrasts with open ocean environments, where pCO_2 variability is small, causing calculated CO_2 fluxes to be particularly sensitive to

variations in k. However, when sufficient wind or current data are available or when k must be resolved over hourly to daily time scales, say for net ecosystem metabolism assessments, it becomes critical to account for spatial-temporal variations in k.

3.6. Impact of Short-Term Variability on Calculated CO_2 Fluxes

To examine the effect of different k parameterizations on CO_2 fluxes over shorter time scales, CO_2 fluxes were calculated over the course of 2 days (Figure 8), one in which diel cycles of wind speed and ΔpCO_2 were typical of a clear summer day (23 August 2017) and another in which pCO_2 and wind speed were relatively stable (30 October 2017). For the day with a large pCO_2 excursion (23 August 2017; Figure 8a), all mass transfer models from this study and from Jiang et al. (2008) tended to underpredict CO_2 flux (relative to EC measurements) before sunrise and after sunset. During these nighttime hours, the ratio of u_{*w}/w_{*w} was also relatively low, between 0.8 and 1.0, indicating that waterside convection was responsible for some fraction of the increased rate of gas transfer. During daylight hours, though, measured and modeled CO_2 flux was generally in good agreement, and no obvious differences existed between the different k_{600} parameterizations used. Furthermore, when CO_2 fluxes were averaged over the full 24-hr period, the effect of different k_{600} parameterizations on calculated CO_2 flux was not significant (one-way Analysis of variance, $\alpha = 0.05$; Figure S2).

During the day with relatively consistent pCO_2 (30 October 2017; Figure 8b), measured and modeled CO_2 fluxes were generally small and negative (i.e., uptake). However, in contrast with 23 August 2017, calculated CO_2 fluxes differed significantly when assessed using different k_{600} parameterizations. This difference is most obvious at 02:00, when calculated CO_2 fluxes ranged from -0.47 mmol·m^{-2}·hr^{-1} (using an average $k_{600} = 9.37$ cm/hr) to -1.43 mmol·m^{-2}·hr^{-1} (when k_{600} was assigned according to day and night binned equations from Table 1). In fact, when CO_2 fluxes were averaged over the entire day, differences between parameterizations were significant, such that the U_{10}-based relationships of Jiang et al. (2008) and our equations (1) and (2) produced CO_2 fluxes that were significantly greater than measured fluxes and significantly less than fluxes determined using an average k_{600} (Figure S2).

4. Conclusion and Recommendations

In this study, we combine direct measurements of both pCO_2 and air-water CO_2 exchange in order to assess the physical forcing of CO_2 flux in the NRE. We fill a current research gap by constructing wind-based k_{600} parameterizations applicable to other shallow and microtidal estuaries. While we were able to define a relationship between wind speed and k_{600}, we found that this relationship is best described by a linear fit during the day and a polynomial fit at night. While it is possible that waterside thermal convection may be responsible for some of this upward inflection in nighttime k at low wind speed, it cannot fully explain this difference. Future studies involving waterside physical measurements may be better suited at identifying the specific mechanism for the observed difference between day and night k. Still, this day-night difference in k was significant and may be of interest in future studies involving highly temporally resolved measurements (e.g., diel studies) or in estuaries where variations in pCO_2 are relatively large. In general, our results suggest that over seasonal to annual time scales, it may be sufficient to simply assume an average k value. While variations in k across estuaries are likely large, the average k_{600} in this study (9.37 cm/hr) compares reasonably well with average k_{600} values from previous studies in estuaries and the open ocean. However, we stress that when shorter time scales are assessed, variations in the shape of the U_{10} versus k relationship must be accounted for. Future studies aimed at more precise measurements of k in estuaries that would be improved by capturing a full annual cycle and including direct measurements of bottom-driven turbulence.

Acknowledgments
We thank SERDP and DCERP for funding and support. Dennis Arbige assisted with EC tower construction, and Susan Cohen provided invaluable logistical support. I also thank Marc Alperin (UNC Chapel Hill) for his thoughtful guidance and encouragement with this project. All data sets for this manuscript are available at FigShare (https://doi.org/10.6084/m9.figshare.7276877.v1). Additional funding for this project was provided by DAAD (57429828) from funds of the German Federal Ministry of Education and Research (BMBF).

References

Abril, G., Commarieu, M. V., Sottolichio, A., Bretel, P., & Guérin, F. (2009). Turbidity limits gas exchange in a large macrotidal estuary. *Estuarine, Coastal and Shelf Science*, *83*(3), 342–348. https://doi.org/10.1016/j.ecss.2009.03.006

Abril, G., Martinez, J.-M., Artigas, L. F., Moreira-Turcq, P., Benedetti, M. F., Vidal, L., et al. (2014). Amazon River carbon dioxide outgassing fuelled by wetlands. *Nature*, *505*(7483), 395–398. https://doi.org/10.1038/nature12797

Andersson, A., Falck, E., Sjöblom, A., Kljun, N., Sahlée, E., Omar, A. M., & Rutgersson, A. (2017). Air-sea gas transfer in high Arctic fjords. *Geophysical Research Letters*, *44*, 2519–2526. https://doi.org/10.1002/2016GL072373

Berg, P., & Pace, M. L. (2017). Continuous measurement of air-water gas exchange by underwater eddy covariance. *Biogeosciences*, *14*, 1–27. https://doi.org/10.5194/bg-14-5595-2017

Borges, A. V. (2005). Do we have enough pieces of the jigsaw to integrate CO_2 fluxes in the coastal ocean? *Estuaries*, *28*(1), 3–27. https://doi.org/10.1007/BF02732750

Borges, A. V., Delille, B., Schiettecatte, L., Gazeau, F., Abril, G., & Frankignoulle, M. (2004). Gas transfer velocities of CO_2 in three European estuaries (Randers Fjord, Scheldt, and Thames). *Limnology and Oceanography*, *49*(5), 1630–1641. https://doi.org/10.4319/lo.2004.49.5.1630

Borges, A. V., Djenidi, S., Lacroix, G., Theate, J., Delille, B., & Frankignoulle, M. (2003). Atmospheric CO_2 flux from mangrove surrounding waters. *Geophysical Research Letters*, *30*(11), 1558. https://doi.org/10.1029/2003GL017143

Broecker, W. S., & Peng, T.-H. (1974). Gas exchange rates between air and sea. *Tellus*, *26*(1–2), 21–35. https://doi.org/10.1111/j.2153-3490.1974.tb01948.x

Cole, J. J., & Caraco, N. F. (1998). Atmospheric exchange of carbon dioxide in a low-wind oligotrophic lake measured by the addition of SF_6. *Limnology and Oceanography*, *43*(4), 647–656. https://doi.org/10.4319/lo.1998.43.4.0647

Cotovicz, L. C., Knoppers, B. A., Brandini, N., Costa Santos, S. J., & Abril, G. (2015). A strong CO_2 sink enhanced by eutrophication in a tropical coastal embayment (Guanabara Bay, Rio de Janeiro, Brazil). *Biogeosciences*, *12*(20), 6125–6146. https://doi.org/10.5194/bg-12-6125-2015

Crosswell, J. R. (2015). Bubble clouds in coastal waters and their role in air-water gas exchange of CO_2. *Journal of Marine Science and Engineering*, *3*(3), 866–890. https://doi.org/10.3390/jmse3030866

Crosswell, J. R., Anderson, I. C., Stanhope, J. W., Van Dam, B., Brush, M. J., Ensign, S., et al. (2017). Carbon budget of a shallow, lagoonal estuary: Transformations and source-sink dynamics along the river-estuary-ocean continuum. *Limnology and Oceanography*, *62*(S1), S29–S45. https://doi.org/10.1002/lno.10631

Crosswell, J. R., Wetz, M. S., Hales, B., & Paerl, H. W. (2014). Extensive CO_2 emissions from shallow coastal waters during passage of Hurricane Irene (August 2011) over the Mid-Atlantic Coast of the U.S.A. *Limnology and Oceanography*, *59*(5), 1651–1665. https://doi.org/10.4319/lo.2014.59.5.1651

Crusius, J., & Wanninkhof, R. (2003). Gas transfer velocities measured at low wind speed over a lake. *Limnology and Oceanography*, *48*(3), 1010–1017. https://doi.org/10.4319/lo.2003.48.3.1010

Edson, J. B., Fairall, C. W., Bariteau, L., Zappa, C. J., Cifuentes-Lorenzen, A., McGillis, W. M., et al. (2011). Direct-covariance measurement of CO_2 gas transfer velocity during the 2008 Southern Ocean gas exchange experiment: Wind speed dependency. *Journal of Geophysical Research*, *116*, C00F10. https://doi.org/10.1029/2011JC007022

Erkkilä, K.-M., Mammarella, I., Bastviken, D., Biermann, T., Heiskanen, J. J., Lindroth, A., et al. (2018). Methane and carbon dioxide fluxes over a lake: Comparison between eddy covariance, floating chambers and boundary layer method. *Biogeosciences Discussions*, *1–29*, 1–29. https://doi.org/10.5194/bg-2017-56

Evans, W., Hales, B., & Strutton, P. G. (2012). pCO2 distributions and air–water CO_2 fluxes in the Columbia River estuary. *Estuarine, Coastal and Shelf Science*, *117*, 260–272. https://doi.org/10.1016/j.ecss.2012.12.003

Frankignoulle, M., Abril, G., Borges, A., Bourge, I., Canon, C., Delille, B., et al. (1998). Carbon dioxide emission from European estuaries. *Science*, *282*(5388), 434–436. Retrieved from http://www.ncbi.nlm.nih.gov/pubmed/9774261, https://doi.org/10.1126/science.282.5388.434

Guo, X., Dai, M., Zhai, W., Cai, W.-J., & Chen, B. (2009). CO_2 flux and seasonal variability in a large subtropical estuarine system, the Pearl River Estuary, China. *Journal of Geophysical Research*, *114*, G03013. https://doi.org/10.1029/2008JG000905

Herrmann, M., Najjar, R. G., Michael, K. W., Alexander, R. B., Boyer, E. W., Cai, W.-J., et al. (2015). Net ecosystem production and organic carbon balance of U.S. East Coast estuaries: A synthesis approach. *Global Biogeochemical Cycles*, *29*, 96–111. https://doi.org/10.1002/2013GB004736

Ho, D. T., Coffineau, N., Hickman, B., Chow, N., Koffman, T., & Schlosser, P. (2016). Influence of current velocity and wind speed on air-water gas exchange in a mangrove estuary. *Geophysical Research Letters*, *43*, 3813–3821. https://doi.org/10.1002/2016GL068727

Ho, D. T., Engel, V. C., Ferrón, S., Hickman, B., Choi, J., & Harvey, J. W. (2018). On factors influencing air-water gas exchange in emergent wetlands. *Journal of Geophysical Research: Biogeosciences*, *123*(1), 178–192. https://doi.org/10.1002/2017JG004299

Ho, D. T., Law, C. S., Smith, M. J., Schlosser, P., Harvey, M., & Hill, P. (2006). Measurements of air-sea gas exchange at high wind speeds in the Southern Ocean: Implications for global parameterizations. *Geophysical Research Letters*, *33*, L16611. https://doi.org/10.1029/2006GL026817

Ho, D. T., Schlosser, P., & Orton, P. M. (2011). On factors controlling air-water gas exchange in a large tidal river. *Estuaries and Coasts*, *34*(6), 1103–1116. https://doi.org/10.1007/s12237-011-9396-4

Jeffery, C. D., Woolf, D. K., Robinson, I. S., & Donlon, C. J. (2007). One-dimensional modelling of convective CO2 exchange in the Tropical Atlantic. *Ocean Modelling*, *19*(3–4), 161–182. https://doi.org/10.1016/j.ocemod.2007.07.003

Jiang, L.-Q., Cai, W.-J., & Wang, Y. (2008). A comparative study of carbon dioxide degassing in river- and marine-dominated estuaries. *Limnology and Oceanography*, *53*(6), 2603–2615. https://doi.org/10.4319/lo.2008.53.6.2603

Kljun, N., Calanca, P., Rotach, M. W., & Schmid, H. P. (2015). A simple two-dimensional parameterisation for flux footprint prediction (FFP). *Geoscientific Model Development*, *8*(11), 3695–3713. https://doi.org/10.5194/gmd-8-3695-2015

Koné, Y. J. M., Abril, G., Kouadio, K. N., Delille, B., & Borges, A. V. (2009). Seasonal variability of carbon dioxide in the rivers and lagoons of Ivory Coast (West Africa). *Estuaries and Coasts*, *32*(2), 246–260. https://doi.org/10.1007/s12237-008-9121-0

Large, W., & Pond, S. (1981). Open ocean momentum flux measurements in moderate to strong winds. *Journal of Physical Oceanography*, *11*(3), 324–336. https://doi.org/10.1175/1520-0485(1981)011<0324:OOMFMI>2.0.CO;2

Laruelle, G. G., Goossens, N., Arndt, S., Cai, W.-J., & Regnier, P. (2017). Air-water CO_2 evasion from U.S. East Coast estuaries. *Biogeosciences*, *14*, 1–54. https://doi.org/10.5194/bg-2016-278

Lee, R. J., & Saylor, J. R. (2010). The effect of a surfactant monolayer on oxygen transfer across an air/water interface during mixed convection. *International Journal of Heat and Mass Transfer*, *53*(17–18), 3405–3413. https://doi.org/10.1016/j.ijheatmasstransfer.2010.03.037

Liang, J.-H., Deutsch, C., McWilliams, J. C., Baschek, B., Sullivan, P. P., & Chiba, D. (2013). Parameterizing bubble-mediated air-sea gas exchange and its effect on ocean ventilation. *Global Biogeochemical Cycles*, *27*, 894–905. https://doi.org/10.1002/gbc.20080

Liu, H., Zhang, Q., Katul, G. G., Cole, J. J., Chapin, F. S., & MacIntyre, S. (2016). Large CO_2 effluxes at night and during synoptic weather events significantly contribute to CO_2 emissions from a reservoir. *Environmental Research Letters*, *11*(6), 64001. https://doi.org/10.1088/1748-9326/11/6/064001

MacIntyre, S., Eugster, W., & Kling, G. W. (2001). The critical importance of buoyancy flux for gas flux across the air-water interface. In M. A. Donelan, W. M. Drennan, E. S. Saltzman, & R. Wanninkhof (Eds.), *Gas Transfer at Water Surfaces*. American Geophysical Union.

MacIntyre, S., Jonsson, A., Jansson, M., Aberg, J., Turney, D. E., & Miller, S. D. (2010). Buoyancy flux, turbulence, and the gas transfer coefficient in a stratified lake. *Geophysical Research Letters*, *37*, L24604. https://doi.org/10.1029/2010GL044164

Maher, D. T., Cowley, K., Santos, I. R., Macklin, P., & Eyre, B. D. (2015). Methane and carbon dioxide dynamics in a subtropical estuary over a diel cycle: Insights from automated in situ radioactive and stable isotope measurements. *Marine Chemistry*, *168*, 69–79. https://doi.org/10.1016/j.marchem.2014.10.017

Maurice, L., Rawlins, B. G., Farr, G., Bell, R., & Gooddy, D. C. (2017). The influence of flow and bed slope on gas transfer in steep streams and their implications for evasion of CO_2. *Journal of Geophysical Research: Biogeosciences*, *122*, 2862–2875. https://doi.org/10.1002/2017JG004045

McDougall, T. J., & Barker, P. M. (2011). *Getting started with TEOS-10 and the Gibbs seawater (GSW) oceanographic toolbox*, *SCOR/IAPSO WG127* (p. 28). Retrieved from http://www.teos-10.org/software.htm

McGillis, W. R., Edson, J. B., Hare, J. E., & Fairall, C. W. (2001). Direct covariance air-sea CO_2 fluxes. *Journal of Geophysical Research*, *106*(C8), 16,729–16,745. https://doi.org/10.1029/2000JC000506

McGillis, W. R., Edson, J. B., Zappa, C. J., Ware, J. D., McKenna, S. P., Terray, E. A., et al. (2004). Air-sea CO_2 exchange in the equatorial Pacific. *Journal of Geophysical Research*, *109*(C8), 1–17. https://doi.org/10.1029/2003JC002256

McKenna, S. P., & McGillis, W. R. (2004). The role of free-surface turbulence and surfactants in air-water gas transfer. *International Journal of Heat and Mass Transfer*, *47*(3), 539–553. https://doi.org/10.1016/j.ijheatmasstransfer.2003.06.001

Mørk, E. T., Sørensen, L. L., Jensen, B., & Sejr, M. K. (2014). Air-sea CO2 gas transfer velocity in a shallow estuary. *Boundary-Layer Meteorology*, *151*(1), 119–138. https://doi.org/10.1007/s10546-013-9869-z

Najjar, R. G., Herrmann, M., Alexander, R., Boyer, E. W., Burdige, D., Butman, D., et al. (2018). Carbon budget of tidal wetlands, estuaries, and shelf waters of Eastern North America. *Global Biogeochemical Cycles*, *32*(3), 389–416. https://doi.org/10.1002/2017GB005790

Pereira, R., Schneider-Zapp, K., & Upstill-Goddard, R. C. (2016). Surfactant control of gas transfer velocity along an offshore coastal transect: Results from a laboratory gas exchange tank. *Biogeosciences*, *13*(13), 3981–3989. https://doi.org/10.5194/bg-13-3981-2016

Podgrajsek, E., Sahlée, E., Bastviken, D., Holst, J., Lindroth, A., Tranvik, L., & Rutgersson, A. (2014). Comparison of floating chamber and eddy covariance measurements of lake greenhouse gas fluxes. *Biogeosciences*, *11*(15), 4225–4233. https://doi.org/10.5194/bg-11-4225-2014

Podgrajsek, E., Sahlée, E., & Rutgersson, A. (2014). Diel cycle of lake-air CO_2 flux from a shallow lake and the impact of waterside convection on the transfer velocity. *Journal of Geophysical Research: Biogeosciences*, *119*, 487–507. https://doi.org/10.1002/2013JG002552. Received

Prytherch, J., Yelland, M. J., Pascal, R. W., Moat, B. I., Skjelvan, I., & Srokosz, M. A. (2010). Open ocean gas transfer velocity derived from long-term direct measurements of the CO_2 flux. *Geophysical Research Letters*, *37*, L23607. https://doi.org/10.1029/2010GL045597

Raymond, P. A., & Cole, J. J. (2001). Gas exchange in rivers and estuaries: Choosing a gas transfer velocity. *Estuaries*, *24*(2), 312–317. https://doi.org/10.2307/1352954

Raymond, P. A., Hartmann, J., Lauerwald, R., Sobek, S., McDonald, C., Hoover, M., et al. (2013). Global carbon dioxide emissions from inland waters. *Nature*, *503*(7476), 355–359. https://doi.org/10.1038/nature12760

Rosentreter, J. A., Maher, D. T., Ho, D. T., Call, M., Barr, J. G., & Eyre, B. D. (2017). Spatial and temporal variability of CO_2 and CH_4 gas transfer velocities and quantification of the CH_4 microbubble flux in mangrove dominated estuaries. *Limnology and Oceanography*, *62*(2), 561–578. https://doi.org/10.1002/lno.10444

Rutgersson, A., Smedman, A., & Sahle, E. (2011). Oceanic convective mixing and the impact on air-sea gas transfer velocity. *Geophysical Research Letters*, *38*, L02602. https://doi.org/10.1029/2010GL045581

Smith, S. (1985). Physical, chemical and biological characteristics of CO_2 gas flux across the air-water interface. *Plant, Cell and Environment*, *8*(6), 387–398. https://doi.org/10.1111/j.1365-3040.1985.tb01674.x

Takahashi, T., Olafsson, J., Goddard, J. G., Chipman, D. W., & Sutherland, S. C. (1993). Seasonal variation of CO_2 and nutrients in the high latitude surface oceans: A comparative study. *Global Biochemical Cycles*, *7*(4), 843–878. https://doi.org/10.1029/93GB02263

Tranvik, L. J., Downing, J. a., Cotner, J. B., Loiselle, S. a., Striegl, R. G., Ballatore, T. J., et al. (2009). Lakes and reservoirs as regulators of carbon cycling and climate. *Limnology and Oceanography*, *54*(6part2), 2298–2314. https://doi.org/10.4319/lo.2009.54.6_part_2.2298

Upstill-Goddard, R. C. (2006). Air–sea gas exchange in the coastal zone. *Estuarine, Coastal and Shelf Science*, *70*(3), 388–404. https://doi.org/10.1016/j.ecss.2006.05.043

Vachon, D., & Prairie, Y. T. (2013). The ecosystem size and shape dependence of gas transfer velocity versus wind speed relationships in lakes. *Canadian Journal of Fisheries and Aquatic Sciences*, *70*(12), 1757–1764. https://doi.org/10.1139/cfjas-2013-0241

Van Dam, B. R., Crosswell, J. R., Anderson, I. C., & Paerl, H. W. (2018). Watershed-scale drivers of air-water CO_2 exchanges in two lagoonal, North Carolina (USA) estuaries. *Journal of Geophysical Research: Biogeosciences*, *123*(1), 271–287. https://doi.org/10.1002/2017JG004243

Van Dam, B. R., Crosswell, J. R., & Paerl, H. W. (2018). Flood-driven CO_2 emissions from adjacent North Carolina estuaries during Hurricane Joaquin (2015). *Marine Chemistry*, *207*, 1–12. https://doi.org/10.1016/J.MARCHEM.2018.10.001

Wanninkhof, R. (1992). Relationship between wind speed and gas exchange. *Journal of Geophysical Research*, *97*(C5), 7373–7382. https://doi.org/10.1029/92JC00188

Wanninkhof, R. (2014). Relationship between wind speed and gas exchange over the ocean revisited. *Limnology and Oceanography: Methods*, *12*(6), 351–362. https://doi.org/10.4319/lom.2014.12.351

Wanninkhof, R., Asher, W. E., Ho, D. T., Sweeney, C., & McGillis, W. R. (2009). Advances in quantifying air-sea gas exchange and environmental forcing. *Annual Review of Marine Science*, *1*(1), 213–244. https://doi.org/10.1146/annurev.marine.010908.163742

Wanninkhof, R., & Mcgillis, W. R. (1999). A cubic relationship between air-sea CO_2 exchange and wind speed. *Geophysical Research Letters*, *26*(13), 1889–1892. https://doi.org/10.1029/1999GL900363

Webb, E. K., Pearman, G. I., & Leuning, R. (1980). Correction of flux measurements for density effects due to heat water vapor transport. *Quarterly Journal of the Royal Meteorological Society*, *106*(447), 85–100. https://doi.org/10.1002/qj.49710644707

Woolf, D. K. (2005). Parametrization of gas transfer velocities and sea-state-dependent wave breaking. *Tellus Series B: Chemical and Physical Meteorology*, *57*(2), 87–94. https://doi.org/10.1111/j.1600-0889.2005.00139.x

Zappa, C. J., McGillis, W. R., Raymond, P. A., Edson, J. B., Hintsa, E. J., Zemmelink, H. J., et al. (2007). Environmental turbulent mixing controls on air-water gas exchange in marine and aquatic systems. *Geophysical Research Letters*, *34*, L10601. https://doi.org/10.1029/2006GL028790